

# Metadata of the chapter that will be visualized online

|                      |   |  |
|----------------------|---|--|
| Series Title         | Progress in Colloid and Polymer Science                                 |  |
| Chapter Title        | Colloid Flow Control in Microchannels and Detection by Laser Scattering |  |
| Chapter SubTitle     |   |  |
| Copyright Year       | 2012  |  |
| Copyright Holder     | Springer-Verlag Berlin Heidelberg                                       |  |
| Corresponding Author | Family Name   | Pagliara   |
|                      | Particle  |  |
|                      | Given Name  | <b>Stefano</b>   |
|                      | Suffix  |  |
|                      | Division  | Cavendish Laboratory   |
|                      | Organization  | University of Cambridge  |
|                      | Address   | Cambridge, UK  |
|                      | Email   | sp608@cam.ac.uk  |
| Author               | Family Name   | Chimerel   |
|                      | Particle  |  |
|                      | Given Name  | <b>Catalin</b>   |
|                      | Suffix  |  |
|                      | Division  | Cavendish Laboratory   |
|                      | Organization  | University of Cambridge  |
|                      | Address   | Cambridge, UK  |
|                      | Email   |  |
| Author               | Family Name   | Aarts  |
|                      | Particle  |  |
|                      | Given Name  | <b>dirk G. A. L.</b>   |
|                      | Suffix  |  |
|                      | Division  | Department of Chemistry, Physical and Theoretical Chemistry Laboratory |
|                      | Organization  | University of Oxford   |
|                      | Address   | Oxford, UK   |
|                      | Email   |  |
| Author               | Family Name   | Langford   |
|                      | Particle  |  |
|                      | Given Name  | <b>Richard</b>   |
|                      | Suffix  |  |
|                      | Division  | Cavendish Laboratory   |
|                      | Organization  | University of Cambridge  |
|                      | Address   | Cambridge, UK  |
|                      | Email   |  |
| Author               | Family Name   | Keyser   |
|                      | Particle  |  |

|              |                         |
|--------------|-------------------------|
| Given Name   | <b>ulrich F.</b>        |
| Suffix       |                         |
| Division     | Cavendish Laboratory    |
| Organization | University of Cambridge |
| Address      | Cambridge, UK           |
| Email        |                         |

---

---

**Abstract**

We introduce a new approach towards the flow control and detection of colloids in microfluidic specimens. We fabricate hybrid polydimethylsiloxane (PDMS)/glass microfluidic chips equipped with parallel micrometer and sub-micrometer channels with different width and thickness. We image and detect the colloid flow direction through the microchannels by coupling laser-light-scattering in a restricted region of a single channel. We control single polymer colloids by means of a computerized pressure-based flow control system and study the Poiseuille flow through channels with different square cross section. We demonstrate the possibility of in situ sensing populations of colloids with different dimensions down to the sub-100 nm scale.

---

## Colloid Flow Control in *Microchannels* and Detection by Laser Scattering

Stefano Pagliara<sup>1</sup>, Catalin Chimere<sup>1</sup>, Dirk G. A. L. Aarts<sup>2</sup>, Richard Langford<sup>1</sup>, and Ulrich F. Keyser<sup>1</sup>

**Abstract** We introduce a new approach towards the flow control and detection of colloids in microfluidic specimens. We fabricate hybrid polydimethylsiloxane (PDMS)/glass microfluidic chips equipped with parallel micrometer and sub-micrometer channels with different width and thickness. We image and detect the colloid flow direction through the microchannels by coupling laser-light-scattering in a restricted region of a single channel. We control single polymer colloids by means of a computerized pressure-based flow control system and study the Poiseuille flow through channels with different square cross section. We demonstrate the possibility of in situ sensing populations of colloids with different dimensions down to the sub-100 nm scale.

### Introduction

Single particle flow control, counting and sizing in fluidic specimens is of paramount importance in environmental, industrial and clinical analysis, on-chip particle synthesis and biological sciences [1]. Micro- and nano-fluidics [2] are emerging technologies that rely on biocompatible and low cost materials and mass production fabrication processes, allow the exploitation of tiny liquid volumes and low analyte concentrations and offer an accurately controllable environment. The most common approach regarding the fabrication of *microfluidic* devices consists of a combination of photo- and soft lithography [3] that generally allows only a 2-dimensional control of the features on a same chip.

Among other technologies for the fabrication of features with variable size on a same chip – such as laser micromachining [4], electron beam and photolithography [5], multi-

layer soft lithography [6], gray-tone lithography [7], stereolithography [8], solid-object printing [9] and template assisted molding [10], focused ion beam (FIB) has a number of advantages such as high sensitivity and direct fabrication in selective areas without any etch mask. FIB milling has been previously exploited for the fabrication of nanofluidic channels [11] and microfluidic devices [12–14].

On the other hand among other single particle detection approaches – such as Coulter counter with nanocapillaries [15], electrical impedance [16], laser-induced fluorescence [17], particle tracking [18] and correlation spectroscopy [19], laser-light-scattering is a well established detection technique that offers a non-invasive tool for the counting of micro- and nano-particles down to the 100 nm scale such as polymer colloids, blood cells and viruses [20–23].

Here we introduce a novel approach toward the control of single sub-micrometer colloids. We fabricate microfluidic devices equipped with parallel channels with different cross section by exploiting *Platinum (Pt)* wires deposited via FIB as templates for soft lithography. We characterize translocations of single particles with size in the range 50–450 nm in terms of event frequency, duration and amplitude by coupling laser scattering in a single channel. *We use channels with different cross section on the same chip to investigate the pressure-driven transport of single polymer colloids with diameter of 300nm.* We demonstrate the in situ sensing of populations of colloids with diameters between 50 and 450 nm.

### Experimental

#### Preparation of Colloidal Suspensions

As test particles for our setup we used polystyrene (PS) nanospheres with mean diameter  $(52 \pm 8)$  nm and  $(457 \pm 11)$  nm (Polysciences, Inc. Warrington, PA) in a 2.67% and

S. Pagliara (✉)

<sup>1</sup>Cavendish Laboratory, University of Cambridge, Cambridge, UK  
e-mail: sp608@cam.ac.uk

<sup>2</sup>Department of Chemistry, Physical and Theoretical Chemistry Laboratory, University of Oxford, Oxford, UK

69 2.63% solids (w/v) aqueous suspension, respectively. In  
 70 addition poly(methyl methacrylate) (PMMA) nanospheres  
 71 with mean diameter of  $(290 \pm 55)$  are synthesized by means  
 72 of emulsion polymerization [24, 25] and dispersed in a  
 73 2.63% solids (w/v) aqueous suspension. The saline buffer  
 74 for the colloidal suspensions is a KCl solution with molarity  
 75 in the range 5–50 mM.

## 76 Chip Fabrication

77 The fabrication of the microfluidic chip consists of three  
 78 steps: [26] (a) the deposition of Pt wires on a Silicon sub-  
 79 strate via FIB followed by (b) the patterning of a photoresist  
 80 layer via photolithography for the realization of a reusable  
 81 mold; (c) the replica molding of the latter in PDMS and the  
 82 chemical bonding on a glass substrate via oxygen plasma  
 83 functionalization for the fabrication of the final disposable  
 84 device. The FIB assisted deposition of the Pt wires is carried  
 85 out with a Cross-beam 1540 FIB/SEM system (Zeiss, Ober-  
 86 kochen, Germany) equipped with a Ga+beam. A typical Pt  
 87 deposition is carried out by using an accelerating voltage of  
 88 30 kV and a beam current of 100 pA. The scanning frequen-  
 89 cies are 20,000 and 200 Hz along the longitudinal and or-  
 90 thogonal wire axis, respectively. For the fabrication of the  
 91 mold, a layer of AZ 9260 (Microchemicals GmbH, Ulm,  
 92 Germany) is deposited via spin coating (2,000 rpm for 30 s)  
 93 on the silicon print master previously cleaned by sonication  
 94 in acetone and isopropyl alcohol. After a 3 min pre-bake step  
 95 at  $115^\circ\text{C}$  to remove the residual solvent, the sample is ex-  
 96 posed to UV light (365–405 nm,  $52 \text{ mW/cm}^2$ ) through a  
 97 quartz mask (Photodata Ltd, Hitchin, UK) selectively coated  
 98 with a thin Chromium film patterned with two symmetrical  
 99 stirrup shapes separated by a  $18 \mu\text{m}$  gap (Fig. 1a) and ending  
 100 with four 2 mm-side square pads. Sample and mask are  
 101 carefully aligned through a MJB4 mask aligner (Karl Suss,  
 102 Garching, Germany) in a way that the central region of the  
 103 wire array is positioned under the  $18 \mu\text{m}$ -gap on the mask  
 104 (Fig. 1b). The sample is exposed for 10 s in hard contact  
 105 mode (by realizing a vacuum around 0.8 Bar between sample  
 106 and mask), developed in a deionized water solution of AZ  
 107 400k developer (4:1 in volume) for 8 min at steps of 2 min  
 108 each and finally rinsed with deionized water and dried with  
 109 nitrogen. The thickness of the obtained photoresist structures  
 110 deposited over the Pt wires (Fig. 1a) is around  $12 \mu\text{m}$  as  
 111 measured by a Dektak stylus profilometer (Veeco, Plain-  
 112 view, NY). The sample is baked at  $60^\circ\text{C}$  for 3 h and left in  
 113 air overnight to allow complete evaporation of the solvent.

114 Replica molding of the device is realized by casting on it  
 115 a 9:1 (base:curing agent) PDMS mixture and in situ curing at  
 116  $60^\circ\text{C}$  for 40 min in oven. A typical device is shown in the  
 117 SEM micrograph of Fig. 1c with the inlet and outlet  
 118 reservoirs separated by a  $18 \mu\text{m}$ -wide and  $12 \mu\text{m}$ -thick  
 119 PDMS wall and connected through three hollow channels

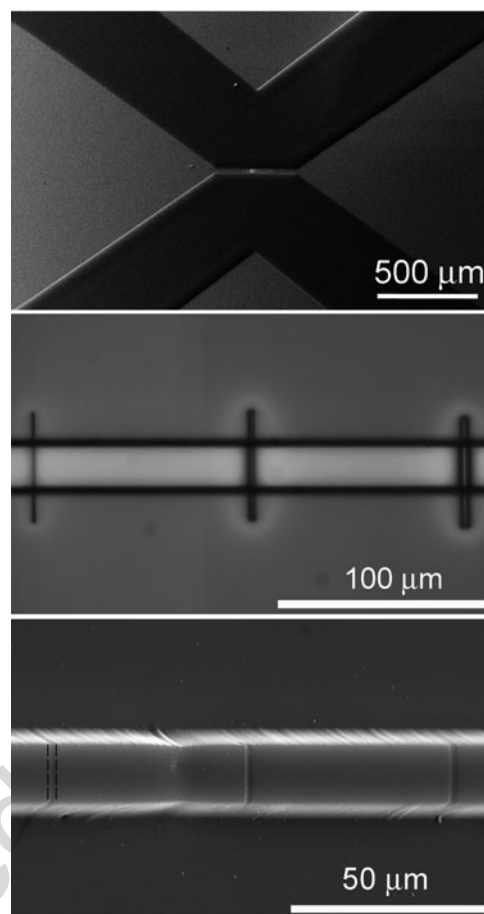


**Fig. 1** (a) Optical micrograph of the mold: two  $12 \mu\text{m}$ -thick symmetrical stirrups made of AZ 9260 are separated by a  $18 \mu\text{m}$  gap. (b) Particular of the  $18 \mu\text{m}$ -long window of uncoated Si and Pt wires with square cross section of 1, 2 and  $3 \mu\text{m}^2$ . (c) SEM micrograph of the resulting PDMS negative replica (tilted at an angle of  $38^\circ$  with respect to the SEM beam column) with hollow channels connecting the inlet and outlet reservoir chambers of the microfluidic chip. Dashed lines mark the smallest channel

with square cross section of 1, 2 and  $9 \mu\text{m}^2$  (from left to right, respectively). Four  $1.5 \text{ mm}$ -wide circular holes are drilled by a  $1.5 \text{ mm}$ -wide circular disposable biopsy punch (Kai Industries Co. Ltd., Seki City, Japan) in correspondence of the four square pads to enable fluidic access to the micro-channels. PDMS is bonded to a glass slide by exposing both surfaces to oxygen plasma treatment ( $8.5 \text{ s}$  exposure to  $2.5 \text{ W}$  plasma power, Plasma etcher, Diener, Royal Oak, MI).  $1.6 \text{ mm}$ -wide PEEK tubing (Kinesis, St Neots, UK) is integrated in the holes exploiting the PDMS flexibility thus ensuring tight and fully sealed connections. The device is completed by the connection to external PEEK shut off valves ( $0.020''$  thru-hole,  $1/16''$  Fittings, Kinesis) on their turn connected to a computerized pressure-based flow control system (maximum applied pressure  $75 \text{ mbar}$ , sub-mbar pressure steps MFCS-4C, Fluigent, Paris, France) that allows to stop and accurately regulate the flow in the microfluidic chip. The pressure gradient is defined as positive when the pressure applied to the inlet is higher than the

120  
121  
122  
123  
124  
125  
126  
127  
128  
129  
130  
131  
132  
133  
134  
135  
136  
137  
138

139 one applied to the outlet. In the same way the translocation  
 140 frequency through the channels is defined as positive when  
 141 the colloids flow from the inlet to the outlet.

### 142 **Detection Set-up**

143 Details about the laser scattering detection set-up are  
 144 reported elsewhere [26]. Briefly a red laser beam is coupled  
 145 into an oil immersion objective and thus focused in a single  
 146 microchannel. The scattered laser-light is coupled to a four  
 147 quadrant photodiode, the voltage signal is amplified and  
 148 digitized. Pressure-driven translocations of colloids appear  
 149 as increases in the voltage trace and are isolated by using a  
 150 custom-made program (LabVIEW 8.6, National Instru-  
 151 ments). Specifically the background signal or baseline is  
 152 calculated every 1,000 points of the trace. The translocation  
 153 events are recorded when a consecutive number of points  
 154 (i.e. 40) exceed twice the value of the baseline standard  
 155 deviation. Translocations of 300 and 50 nm particles through  
 156 a microchannel with square cross section of  $1.4 \mu\text{m}^2$  are  
 157 reported in Fig. 2a and b, respectively. Each single isolated  
 158 event is fitted by a Gaussian curve (solid lines in Fig. 2c and  
 159 d, respectively) which allows determination of the duration  
 160 and amplitude of the translocation event (horizontal and  
 161 vertical arrows, respectively, in Fig. 2b and d), the time  
 162 difference with the previous event and the *signal/noise*  
 163 (*S/N*) ratio. It is noteworthy to observe that the average  
 164 measured *signal/noise* ratio and the time difference between  
 165 two successive events decreases from 60 to 4 and from 350 to  
 166 50 ms, respectively, for particle diameters of 300 and 50 nm.  
 167 The lower *S/N* is due to the decreased amplitude in the signal  
 168 that is reflected back into the objective from the smaller  
 169 particle surface, while the shorter interval within two suc-  
 170 cessive events is due to the presence of a higher number of  
 171 particles,  $10^{11}$  and  $4 \times 10^8 \text{ cm}^{-3}$  for 50 and 300 nm popula-  
 172 tions, respectively.

### 173 **Results**

174 We investigated the pressure-driven colloid transport  
 175 through channels with different square cross section. We  
 176 carried out experiments on two different devices each  
 177 equipped with an array of three channels with cross section  
 178 of 0.4, 1.4,  $3.2 \mu\text{m}^2$  and 1, 4,  $9 \mu\text{m}^2$ , respectively. We  
 179 measure the *translocation frequency* of 300 nm particles  
 180 with respect to the channel cross section (Table 1) under  
 181 an applied pressure gradient of 40 mbar. The general de-  
 182 scription of hydrodynamic phenomena by the Navier-Stokes  
 183 equation reduces in most of the microfluidic systems to the  
 184 linear Stokes equation and the so called Stokes or creeping

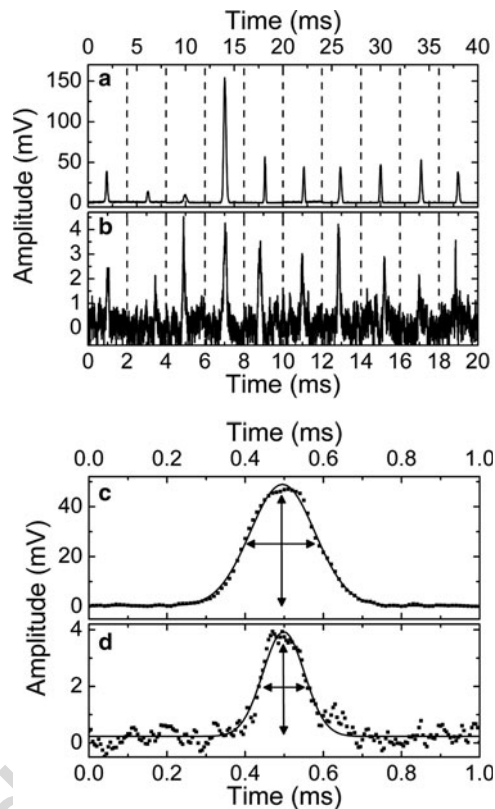


**Fig. 2** Selected intervals of 4 (a) and 2 ms (b) showing ten single events isolated from the voltage traces of 300 (a) and 50 nm colloids (b) translocating a microchannel with square cross section of  $1.4 \mu\text{m}^2$ . Measured signal of a single event (squares) fitted by a Gaussian curve (solid lines) with the estimation of translocation duration and amplitude (horizontal and vertical arrows) for 300 nm (c) and 50 nm (d) colloids

185 flow since in the limit of low Reynolds numbers the non-  
 186 linear term can be neglected [27]. In particular the particle  
 187 flow in closed channel systems can be described by intro-  
 188 ducing the channel and particle Reynolds numbers (Table 1),  
 189  $Re_c$  and  $Re_p$ : [28]

$$Re_c = \frac{U_m \sqrt{S} \rho}{\eta}, \quad Re_p = \frac{U_m d^2 \rho}{\eta \sqrt{S}} \quad (1)$$

190 where  $U_m$  is the maximum velocity of the channel flow,  $S$  is  
 191 the channel cross section,  $d$  is the particle diameter,  $\eta$  and  $\rho$   
 192 the dynamic viscosity and density of the flowing solution.  
 193 The small values of the channel Reynolds number (Table 1)  
 194 indicate that the non-linear term is negligible. In particular  
 195 the pressure-driven, steady-state flow through long, straight  
 196 and rigid microchannels with square cross section can be  
 197 described by the Hagen-Poiseuille flow that predicts a sec-  
 198 ond power law of the volumetric flow rate,  $Q$ , with respect to  
 199  $S$ : [27]

$$Q \approx 0.27 \frac{\Delta p}{12\eta L} S^2 \quad (2)$$

t1.1 **Table 1** Microchannel cross section  $S$ , measured  $f_m$  and predicted  $f_p$  translocation frequencies and corresponding errors. The error in  $S$  is evaluated by considering a 100 nm uncertainty in the SEM measurement of the channel width and height. The errors in  $f_m$  is the standard deviation calculated by averaging over measurements acquired for an interval of 30 s. For the error in  $f_p$  we take into account the error in  $S$  and a  $\sim 100$  nm uncertainty in the diameter of the laser spot. The values refer to experiments with 300 nm particles

| t1.2 | $S$ ( $\mu\text{m}^2$ ) | $Re_c$ | $Re_p$              | $\omega$ ( $\text{s}^{-1}$ ) | $f_m$ (s)     | $f_p$ (s)      |
|------|-------------------------|--------|---------------------|------------------------------|---------------|----------------|
| t1.3 | $0.4 \pm 0.1$           | 0.001  | $3.1 \cdot 10^{-4}$ | $2 \cdot 10^3$               | $0.5 \pm 0.1$ | $0.3 \pm 0.2$  |
| t1.4 | $1 \pm 0.2$             | 0.007  | $6.1 \cdot 10^{-4}$ | $3 \cdot 10^3$               | $0.9 \pm 0.3$ | $2.5 \pm 1$    |
| t1.5 | $1.4 \pm 0.2$           | 0.012  | $7.7 \cdot 10^{-4}$ | $4 \cdot 10^3$               | $3 \pm 0.4$   | $4.3 \pm 1.6$  |
| t1.6 | $3.2 \pm 0.4$           | 0.040  | $1.1 \cdot 10^{-3}$ | $6 \cdot 10^3$               | $5.2 \pm 0.6$ | $6.5 \pm 2.2$  |
| t1.7 | $4 \pm 0.4$             | 0.055  | $1.2 \cdot 10^{-3}$ | $7 \cdot 10^3$               | $8.6 \pm 1$   | $7.2 \pm 2.4$  |
| t1.8 | $9 \pm 0.6$             | 0.184  | $1.8 \cdot 10^{-3}$ | $10^4$                       | $9.3 \pm 0.9$ | $10.8 \pm 3.4$ |

200 where  $L$  is the channel length and  $\Delta p$  is the pressure gradient.  
 201 For a square cross section the error of this approximate result  
 202 is around 13% [27]. At the connection between the reservoirs  
 203 and the microchannels the Poiseuille description is still  
 204 approximately correct since  $Re_c$  remains  $\leq 1$  which means  
 205 that the non-linear term in the Navier-Stokes equation has a  
 206 vanishingly small contribution and that the inertia effect at  
 207 the microchannel inlet are negligible. Moreover the laser  
 208 detection was coupled in the central part of each micro-  
 209 channel far away from the channel inlet and outlet. For  
 210 particles dispersed in low concentration dispersion, particle  
 211 flow is described by the fluid flow. In fact, since the particle  
 212 Reynolds number (Table 1) is small particle flow is domi-  
 213 nated by viscous drag of the fluid [27, 28]. Therefore the  
 214 predicted translocation frequency can be described as:

$$f_p = nQ = n \frac{\Delta p}{12\eta L} 0.37S^2 \quad (3)$$

215 where  $n$  is the number of particles per unit volume, which is  
 216 estimated to be  $4.2 \times 10^8 \text{ cm}^{-3}$ .

217 Moreover inertial effects such as the lift and drag force  
 218 play a negligible role and the flow remains laminar [28, 29].  
 219 It is noteworthy to observe that the flowing particles rotate  
 220 following the fluid vorticity [30]. In fact in a Newtonian fluid  
 221 in shear flow with no-slip boundary conditions imposed on  
 222 the surface of the sphere, the rotation speed of a single  
 223 particle,  $\omega$ , is given by: [30]

$$\omega = \frac{\dot{\gamma}}{2} \quad (4)$$

224 where  $\dot{\gamma}$  is the shear rate [31]. Typical rotation speed are  
 225 reported in Table 1. No shear thickening [32] is expected  
 226 since the suspended colloids occupy only a volume fraction  
 227 down to  $10^{-6}$ .

228 For an applied pressure gradient of  $\Delta p = 40$  mbar and  
 229 taking into account that for large channels ( $S > 1.1 \mu\text{m}^2$ )

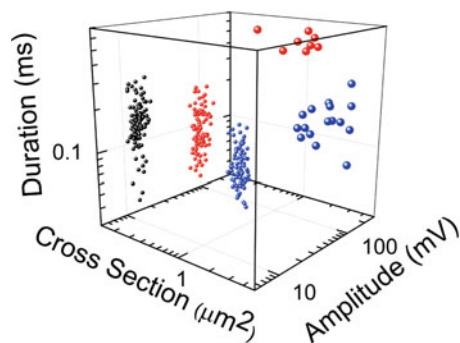


**Fig. 3** 3D scatter plot reporting duration and amplitude of 100 translocations of 50 and 450 nm colloids (small and large spheres, respectively) through channels with square cross section of 0.4, 1.4, 3.2  $\mu\text{m}^2$  (black, red and blue spheres, respectively)

the laser spot,  $a$ , occupies only a fraction of the microchan- 230  
 231 nel volume:

$$f_p = 2.86S^2 \text{ Hz}/\mu\text{m}^4 \text{ for } S 1.1 \mu\text{m}^2$$

$$f_p = 2.86\sqrt{S} \frac{4}{3}\pi a^3 \text{ Hz}/\mu\text{m}^4 \text{ for } S 1.1 \mu\text{m}^2 \quad (5)$$

The translocation frequency,  $f_p$ , predicted by (5) repro- 232  
 233 duces the measured translocation frequency,  $f_m$ , within the  
 234 error bars (Table 1).

Therefore the laser scattering set-up coupled into a single 235  
 236 channel provides quantitative information about the transport  
 237 of particles with diameters of a few hundreds of nanometers.  
 238 Moreover the presented platform allows the sensing of parti-  
 239 cles with diameter down to the 50 nm scale. In particular the  
 240 sensing of particles over a range of diameters is easily  
 241 achieved by exploiting channels with different cross section  
 242 on the same microfluidic chip. As a proof of concept 50 nm  
 243 particles are initially injected in the chip and detected in three  
 244 different channels with cross section 0.4, 1.4, 3.2  $\mu\text{m}^2$ . There-  
 245 after a small amount of 450 nm particles (around 1:100 w/w  
 246 ratio with respect to the 50 nm ones) is injected and the  
 247 translocations of both types of particles are recorded. The  
 248 biggest particles reach the outlet reservoir by going through  
 249 the medium and the biggest channels (red and blue large  
 250 spheres) but do not travel across the smallest channel as high-  
 251 lighted in the scatter plot in Fig. 3. In fact both small (ampli-  
 252 tude  $< 10$  mV) and big particles (amplitude  $> 30$  mV) are  
 253 detected in the two former channels while only small particles  
 254 (black small spheres) are detected in the latter one. Therefore  
 255 by simply looking at the scattering events in different channels  
 256 in the same chip one can easily detect populations of particles  
 257 over a range of diameters.

The presented novel microfluidic platform can be readily 258  
 259 exploited to investigate the interactions between the flowing  
 260 particles and the device surface by studying the transport

261 parameters (i.e. event frequency, amplitude, duration) as a  
 262 function of the salt concentration. *We are currently explor-*  
 263 *ing the possibility of employing such microfluidic systems to*  
 264 *mimic the diffusion of metabolites across membrane protein*  
 265 *pores and to investigate and model the physics of single*  
 266 *channel transport. Further tuning of the glass/PDMS sur-*  
 267 *faces through polymer or protein coating may be required*  
 268 *for more specific biological applications such as the inves-*  
 269 *tigation of DNA translocations under concentration/pH*  
 270 *gradient or electro-phoretic/osmosis force [15]. The exploi-*  
 271 *tation of stiffer material extensively used in soft lithography*  
 272 *for the generation of 50 nm features [33] could open the way*  
 273 *for the realization of nanochannels for nanofluidics while the*  
 274 *improvement of the detection set-up for example with the*  
 275 *integration of a high speed nanoscanning piezostage could*  
 276 *allow the investigation of the transport of particles with*  
 277 *diameter down to the sub-50 nm scale.*

## 278 Conclusions

279 We have proposed a simple and versatile approach for the  
 280 control of sub-micrometer colloids in polymer-based lab-on-  
 281 a-chip systems equipped with arrays of parallel channels  
 282 with different square cross section down to  $0.4 \mu\text{m}^2$ . We  
 283 have coupled laser scattering in single microchannels for the  
 284 in situ detection of single translocating colloids with mini-  
 285 mum detectable particle size of 50 nm. We demonstrate that  
 286 the pressure-driven transport of 300 nm particles through  
 287 channels with different cross section can be modeled by a  
 288 Poiseuille flow. Finally we demonstrated the sensing of  
 289 particles with different diameters by exploiting channels  
 290 with a range of cross sections on the same microfluidic chip.

## 291 References

- 292 1. Zhang H, Chon CH, Pan X, Li D (2009) *Microfluid Nanofluid*  
 293 7:739  
 294 2. Salieb-Beugelaar GB, Simone G, Arora A, Philippi A, Manz A  
 295 (2010) *Anal Chem* 82:4848

3. Duffy DC, McDonald JC, Schueller OJA, Whitesides GM (1998) *Anal Chem* 70:4974 296  
 4. Wolfe DB, Ashcom JB, Hwang JC, Schaffer CB, Mazur E, Whitesides GM (2003) *Adv Mater* 15:62 297  
 5. Jung S-Y, Retterer ST, Collier CP (2010) *Lab Chip* 10:2688 298  
 6. Wu H, Odom TW, Chiu DT, Whitesides GM (2003) *J Am Chem Soc* 125:554 299  
 7. Chung J, Hsu W (2007) *J Vac Sci Technol B* 25:1671 300  
 8. Mizukami Y, Rajniak D, Rajniak A, Nishimura M (2002) *Sens Actuat B-Chem* 81:202 301  
 9. McDonald JC, Chabinyc ML, Metallo SJ, Anderson JR, Stroock AD, Whitesides GM (2002) *Anal Chem* 74:1537 302  
 10. Tu D, Pagliara S, Camposeo A, Potente G, Mele E, Cingolani R, Pisignano D (2011) *Adv Funct Mater* 21:1140 303  
 11. Maleki T, Mohammadi S, Ziaie B (2009) *Nanotechnology* 20:105302 304  
 12. Campbell LC, Wilkinson MJ, Manz A, Camilleri P, Humphreys CJ (2004) *Lab Chip* 4:225 305  
 13. Imre A, Ocola LE, Rich L, Klingfus J (2010) *J Vac Sci Technol B* 28:304 306  
 14. Wanzenboeck HD, Fischer M, Mueller S, Bertagnolli E (2004) *Proc IEEE Sens* 1-3:227 307  
 15. Steinbock LJ, Otto O, Chimere C, Gornall J, Keyser UF (2010) *Nano Lett* 10:2493 308  
 16. Segerink LI, Sprenkels AdJ, ter Braak PM, Vermes I, van den Berg A (2010) *Lab Chip* 10:1018 309  
 17. Andreyev D, Arriaga EA (2007) *Anal Chem* 79:5474 310  
 18. Otto O, Czerwinski F, Gornall JL, Stober G, Oddershede LB, Seidel R, Keyser UF (2010) *Opt Express* 18:22722 311  
 19. Gadd JC, Kuyper CL, Fujimoto BS, Allen RW, Chiu DT (2008) *Anal Chem* 80:3450 312  
 20. Kummrow A, Theisen J, Frankowski M, Tuchscheerer A, Yildirim H, Brattke K, Schmidt M, Neukammer J (2009) *Lab Chip* 9:972 313  
 21. Pamme N, Koyama R, Manz A (2003) *Lab Chip* 3:187 314  
 22. Steen HB (2004) *Cytometry A* 57A:94 315  
 23. Rezenom YH, Wellman AD, Tilstra L, Medley CD, Gilman SD (2007) *Analyst* 132:1215 316  
 24. O'Callaghan KJ, Paine AJ, Rudin A (2007) *J Appl Polym Sci* 1995:58 317  
 25. Kumacheva E, Kalinina O, Lilje L (1999) *Adv Mater* 11:231 318  
 26. Pagliara S, Chimere C, Aarts DGAL, Langford R, Keyser UF *Lab Chip*. doi:10.1039/c1lc20399a 319  
 27. Bruus H (2008) *Theoretical microfluidics*. Oxford University Press, Oxford 320  
 28. Di Carlo D, Irimia D, Tompkins RG, Toner M (2007) *Proc Nat Acad Sci USA* 104:18892 321  
 29. Kim YW, Yoo JY (2008) *J Micromech Microeng* 18:065015 322  
 30. Snijkers F, D'Avino G, Maffettone PL, Greco F, Hulsen M, Vermant J (2009) *J Rheol* 53:459 323  
 31. Girardo S, Cingolani R, Pisignano D (2007) *Anal Chem* 79:5856 324  
 32. Lee YS, Wagner NJ (2003) *Rheol Acta* 42:199 325  
 33. Odom TW, Love JC, Wolfe DB, Paul KE, Whitesides GM (2002) *Langmuir* 18:5314 326  
 327  
 328  
 329  
 330  
 331  
 332  
 333  
 334  
 335  
 336  
 337  
 338  
 339  
 340  
 341  
 342  
 343  
 344  
 345  
 346  
 347  
 348